SIMULATION OF *I-V* AND *C-V* CURVES OF metal/GaN/AlGaN/GaN HETEROSTRUCTURES WITH TRAP-ASSISTED TUNNELLING

Juraj Racko[1], Peter Benko[1], Alena Grmanová[1], Ralf Granzner[2], Frank Schwierz[2], Ladislav Harmatha[1], Juraj Breza[1]

[1] Slovak University of Technology, Ilkovičova 3, 812 19 Bratislava, Slovakia
[2] Technical University Ilmenau, PF 986684, Ilmenau, Germany
E-mail: juraj.breza@stuba.sk

Received 10 May 2013; accepted 16 May 2013

1. Theory

The studied structure and considered exchange processes are shown in Fig. 1. The physical model is based on solving the Poisson and continuity equations. The Poisson equation can be written as

$$-\frac{\mathrm{d}}{\mathrm{d}x}\left(\kappa(x)\frac{\mathrm{d}\psi(x)}{\mathrm{d}x}\right)=\rho(x)=q\Big(p(x)-n(x)+N^{\mathrm{D}+}(x)-N^{\mathrm{A}-}(x)+N_{\mathrm{t}}^{\mathrm{D}+}(x)-N_{\mathrm{t}}^{\mathrm{A}-}(x)\Big), \qquad (1)$$

where κ is the permittivity, ψ is the electric potential, n and p are concentrations of free charge carriers, $N^{\mathrm{D}+}$ and $N^{\mathrm{A}-}$ are concentrations of shallow ionized donors and acceptors, and $N_{\mathrm{t}}^{\mathrm{D}+}$ and $N_{\mathrm{t}}^{\mathrm{A}-}$ are concentrations of deep ionized donors and acceptors expressed as

$$N_{\mathrm{t}}^{\mathrm{D}+}(x)=\int_{E_{\mathrm{V}}(x)}^{E_{\mathrm{C}}(x)} D_{\mathrm{t}}^{\mathrm{D}}(x,\varepsilon)\big(1-f(x,\varepsilon)\big)\mathrm{d}\varepsilon\,, \qquad N^{\mathrm{A}-}(x)=\int_{E_{\mathrm{V}}(x)}^{E_{\mathrm{C}}(x)} D_{\mathrm{t}}^{\mathrm{A}}(x,\varepsilon)f_{\mathrm{t}}(x,\varepsilon)\mathrm{d}\varepsilon\,. \qquad (2, 3)$$

Here, f_{t} is the occupation probability of trapping centres lying at deep energy levels. Definition of the distribution functions of traps in the forbidden band, $D_{\mathrm{t}}^{\mathrm{D,A}}$, based on the theory of multiphonon assisted tunnelling, can be found in [1, 2]. The distribution is given as [3]

$$D_{\mathrm{t}}(\varepsilon,x)=\frac{N_{\mathrm{t}}}{\sqrt{2\pi}\varepsilon_{\mathrm{r}}}\frac{(\theta\mp S)^2}{\left(\theta^2+z^2\right)^{\frac{1}{4}}}\exp\left(\sqrt{z^2+\theta^2}-\theta\ln\left(\frac{\theta}{z}+\sqrt{1+\left(\frac{\theta}{z}\right)^2}\right)-S\big(2f_{\mathrm{B}}+1\big)-\frac{|\varepsilon-E_{\mathrm{t}}|}{2kT}\right), \quad (4)$$

where S is the Huang-Rhys factor representing the strength of electron-phonon coupling, $\varepsilon_{\mathrm{r}}=S\hbar\omega_0$ is the lattice relaxation energy, $\hbar\omega_0$ is the effective phonon energy, $\theta=\frac{|\varepsilon-E_{\mathrm{t}}|}{\hbar\omega_0}$, $f_{\mathrm{B}}=\left(\exp\left(\frac{\hbar\omega_0}{kT}\right)-1\right)^{-1}$ is the Bose distribution function, and $z=2S\sqrt{f_{\mathrm{B}}(1+f_{\mathrm{B}})}$.
The sign inside the bracket in the nominator is negative for $\varepsilon>E_{\mathrm{C}}(x)-E_{\mathrm{t}}$ and positive for $\varepsilon<E_{\mathrm{C}}(x)-E_{\mathrm{t}}$.

The Poisson equation is solvable satisfying the hetero-interface condition

$$\kappa_{\mathrm{GaN}}\left.\frac{\mathrm{d}\psi}{\mathrm{d}x}\right|_{\mathrm{interface}}-\kappa_{\mathrm{AlGaN}}\left.\frac{\mathrm{d}\psi}{\mathrm{d}x}\right|_{\mathrm{interface}}=Q_{\mathrm{het}1,2}\,, \qquad (5)$$

where $Q_{\mathrm{het}1,2}$ is the overall charge at the upper (GaN/AlGaN) or lower (AlGaN/GaN) junction, expressed as a sum of spontaneous and piezoelectric polarization [3-5]. The continuity equations for electrons and holes can be written as

$$\frac{\mathrm{d}J_{\mathrm{D}}^{\mathrm{e}}}{q\mathrm{d}x} = U_{\mathrm{GR}}^{\mathrm{e}} = U_{\mathrm{SRH}} + U_{\mathrm{TAT}}^{\mathrm{e(THER)}} + U_{\mathrm{TAT}}^{\mathrm{e(TUN)}}, \qquad -\frac{\mathrm{d}J_{\mathrm{D}}^{\mathrm{h}}}{q\mathrm{d}x} = U_{\mathrm{GR}}^{\mathrm{h}} = U_{\mathrm{SRH}}. \tag{6}$$

Here, U_{SRH}, $U_{\mathrm{TAT}}^{\mathrm{e(THER)}}$ and $U_{\mathrm{TAT}}^{\mathrm{e(TUN)}}$ are electron recombination rates of trap-assisted tunnelling.

The model of trap-assisted tunnelling (TAT) introduces the concepts of thermal and tunnelling escape times [3].

Fig. 1: *Eight exchange processes considered in the model of trap-assisted tunnelling in a reverse biased* metal/GaN/Al_xGaN_{1-x}/GaN *heterostructure at* $V_{\mathrm{a}}=-2$ V.

The formulae for calculating the thermal escape times are

$$\left(\tau_{\mathrm{R}}^{\mathrm{e}}(x)\right)^{-1} = \mathrm{v}_{\mathrm{th}}^{\mathrm{e}}\sigma_{\mathrm{t}}n(x), \qquad \left(\tau_{\mathrm{G}}^{\mathrm{e}}(x)\right)^{-1} = \mathrm{v}_{\mathrm{th}}^{\mathrm{e}}\sigma_{\mathrm{t}}N_{\mathrm{C}}\exp\left(\left(\varepsilon - E_{\mathrm{C}}(x)\right)/kT\right), \tag{7, 8}$$

$$\left(\tau_{\mathrm{R}}^{\mathrm{h}}(x)\right)^{-1} = \mathrm{v}_{\mathrm{th}}^{\mathrm{h}}\sigma_{\mathrm{t}}p(x), \qquad \left(\tau_{\mathrm{G}}^{\mathrm{h}}(x)\right)^{-1} = \mathrm{v}_{\mathrm{th}}^{\mathrm{h}}\sigma_{\mathrm{t}}N_{\mathrm{V}}\exp\left(\left(E_{\mathrm{V}}(x) - \varepsilon\right)/kT\right), \tag{9, 10}$$

and those for the tunnelling escape times

$$\left(\tau_{\mathrm{CBT}}^{\mathrm{e_right,\,left}}(x,\varepsilon)\right)^{-1} = \frac{m_{\mathrm{R}}^{\mathrm{e}}\sigma_{\mathrm{t}}}{2\pi^2\hbar^3}(\Delta\varepsilon)^2\sum_{j=0}^{N} j\exp\left(-\frac{\sqrt{8m_{\mathrm{T}}^{\mathrm{e}}}}{\hbar}\int_{x,x_{\varepsilon}^{\mathrm{left}}}^{x_{\varepsilon}^{\mathrm{right}},x}\sqrt{E_{\mathrm{C}}(x) - \varepsilon + j\Delta\varepsilon}\,\mathrm{d}x\right), \tag{11}$$

$$\left(\tau_{\mathrm{MT}}^{\mathrm{e}}(x,\varepsilon)\right)^{-1} = \frac{m_{\mathrm{R}}^{\mathrm{e}}\sigma_{\mathrm{t}}}{2\pi^2\hbar^3}(\Delta\varepsilon)^2\sum_{j=0}^{N} j\exp\left(-\frac{\sqrt{8m_{\mathrm{T}}^{\mathrm{e}}}}{\hbar}\int_{x_{\mathrm{M}}}^{x}\sqrt{E_{\mathrm{C}}(x) - \varepsilon + j\Delta\varepsilon}\,\mathrm{d}x\right), \tag{12}$$

where $\Delta\varepsilon$ is the energy increment. Summation of the series terminates, when the ratio of the exponential term for $j=N$ to that for $j=0$ is smaller than a chosen accuracy, e.g., 10^{-6}, σ_{t} is the effective trap cross-section, $m_{\mathrm{R}}^{\mathrm{e}}$ is the effective mass for calculating the Richardson constant in the semiconductor, $m_{\mathrm{T}}^{\mathrm{e}}$ is the effective tunnelling mass of electrons, $\mathrm{v}_{\mathrm{th}}^{\mathrm{e,h}} = \sqrt{3kT/m_{\mathrm{e,h}}^{*}}$ are thermal velocities of charge carriers. In terms of these escape times we derive the probability of occupation of the trap by electrons valid for the range of energies $\varepsilon \in (E_{\mathrm{v}}(x_{\mathrm{M}}), E_{\mathrm{c}}(x_{\mathrm{M}}))$

$$f_t(x,\varepsilon) = \frac{\frac{1}{\tau_R^e} + \frac{1}{\tau_G^h} + \frac{f_{F_n}(x_\varepsilon^{right})}{\tau_{CBT}^{e_right}} + \frac{f_M}{\tau_{MT}^e}}{\frac{1}{\tau_R^e} + \frac{1}{\tau_G^e} + \frac{1}{\tau_G^h} + \frac{1}{\tau_R^h} + \frac{1}{\tau_{CBT}^{e_right}} + \frac{1}{\tau_{MT}^e}} \tag{13}$$

and for the range of energies $\varepsilon \in (E_c(x_M), E_c(x_{het1}))$

$$f_t(x,\varepsilon) = \frac{\frac{1}{\tau_R^e} + \frac{1}{\tau_G^h} + \frac{f_{F_n}(x_\varepsilon^{right})}{\tau_{CBT}^{e_right}} + \frac{f_{F_n}(x_\varepsilon^{left})}{\tau_{CBT}^{e_left}}}{\frac{1}{\tau_R^e} + \frac{1}{\tau_G^e} + \frac{1}{\tau_G^h} + \frac{1}{\tau_R^h} + \frac{1}{\tau_{CBT}^{e_right}} + \frac{1}{\tau_{CBT}^{e_left}}}. \tag{14}$$

Here, $x_\varepsilon^{right}, x_\varepsilon^{left}$ are positions of the right and left intersections of energy level ε with $E_C(x)$, f_{F_n} and f_M are the Fermi-Dirac distribution functions for electrons in the semiconductor and metal, respectively. Details were published in [4], where the formulae are given for calculating U_{SRH}, $U_{TAT}^{e(THER)}$ and $U_{TAT}^{e(TUN)}$. The electron and hole drift-diffusion current densities in the continuity equations are defined as

$$J_D^e = -q\mu^e(x)\left(n(x)\frac{d\psi^e(x)}{dx} - \frac{kT}{q}\frac{dn(x)}{dx}\right), \quad J_D^h = -q\mu^h(x)\left(p(x)\frac{d\psi^h(x)}{dx} + \frac{kT}{q}\frac{dp(x)}{dx}\right). \tag{15, 16}$$

In the case of the heterostructure, the electron and hole electric potentials are

$$\psi^{e,h}(x) = \psi(x) \pm \frac{\Delta E_{C,V}(x)}{q} \pm \frac{kT}{q}\ln\left(n_{C,V}(x)n_{ie}(x)\gamma^{e,h}(x)\right). \tag{17}$$

In these expressions, $n_C(x) = N_C(x)/N_C(x_{GaN})$, $n_V(x) = N_V(x)/N_V(x_{GaN})$, the electron band offset $\Delta E_C(x) = \chi(x_{GaN}) - \chi(x)$ is defined as a difference in electron affinities, the hole band offset $\Delta E_V(x) = E_g(x) - E_g(x_{GaN}) - \Delta E_C(x)$, $\gamma^{e,h}$ transforms the Boltzmann statistics into the Fermi-Dirac statistics and n_{ie} accounts for bandgap narrowing [5]. To solve the continuity equation it is required to define the boundary and interface conditions. The electron density at the metal/GaN interface $n_0(x_M)=N_C\exp(-\phi_b/kT)$ depends on the Schottky barrier height ϕ_b. At the back side of the structure, $x=x_L$, we considered an ohmic contact with a constant electron concentration $n(x_L)=N^{D+}(x_L)$.

In the metal/GaN/Al_xGaN_{1-x}/GaN structure we will consider only the electron component of the current. The hole current can be neglected. The total electron current density $J^e(V_a)$ flowing through the structure on applying voltage V_a is affected by the barrier at the first heterojunction. Under thermodynamic equilibrium, this barrier is higher than the Schottky barrier at the metal/GaN interface and becomes lower on applying a reverse bias. The *I-V* and *C-V* curves are calculated as

$$J^e(V_a) = q\frac{N_i\left(\exp\left(\frac{V_a}{V_t}\right)-1\right) + \frac{1}{V_t}\int_{x_0}^{x_L}\frac{J_{GR}^e(x)}{\mu^e(x)}\exp\left(-\frac{\psi^e(x)}{V_t}\right)dx}{\frac{1}{V_t}\int_{x_0}^{x_L}\frac{1}{\mu^e(x)}\exp\left(-\frac{\psi^e(x)}{V_t}\right)dx}, \quad C(V_a) = \frac{d\int_{x_M}^{x_L}\rho(x)dx}{dV_a}, \tag{18, 19}$$

where $J_{GR}^e(x) = q\int_{x_M}^{x} U_{GR}^e(x')dx'$ is the generation-recombination current density.

2. Simulations

The model was employed to simulate metal/GaN/Al$_x$GaN$_{1-x}$/GaN Schottky heterostructures with molar concentrations of aluminium $x = 0.15$, and with a Schottky barrier height $\phi_b = 0.8$ eV. The vertical geometry of the structure along with the concentration profile of ionized shallow donors $N^{D+}(x)$ is given in Tab. 1. The concentration of traps was assumed to be $N_t = 5\times10^{17}$ cm^{-3} at energy level E_t placed 0.55 eV below the conduction band, thus $E_C - E_t = 0.55$ eV.

Tab. 1: *Vertical geometry of the simulated structure.*

	Cover GaN	Doped AlGaN	Undoped GaN	Doped GaN
Thickness (nm)	5	20	50	20
N^{D+} (cm^{-3})	10^{14}	10^{18}	10^{14}	10^{18}

In simulations taking into account trap-assisted-tunnelling we considered the Huang-Rhys factor S=3.25 and effective phonon energy $\hbar\omega_0$=0.033 eV. The effective cross section was set constant $\sigma_t = 10^{-13}$ cm^2. For calculating the tunnelling escape times τ_{CBT} and τ_{MT}, effective masses $m_R^e = m_T^e = 0.19\,m_0$ were used. The overall charge Q_{het1} at the upper (GaN/AlGaN) junction is negative, Q_{het2} at the lower (AlGaN/GaN) junction is positive and the value of the charge is a material parameter depending on the molar concentration x of aluminium, $Q_{het1,2} = \mp Q_{het}(x)$. Selected parameters depending on the molar concentration of aluminium [6, 7] are summarized in Tab. 2.

Tab. 2: *Parameters depending on the molar concentration of aluminium in the* metal/GaN/AlGaN/GaN *structure.*

$Q_{het\,1,2}$ (As/cm^2)	ΔE_C (eV)	ΔE_V (eV)	$\kappa_{AlGaN} / \kappa_{GaN}$
$\mp 2.16\times10^{-6}$	0.419	0.084	0.975

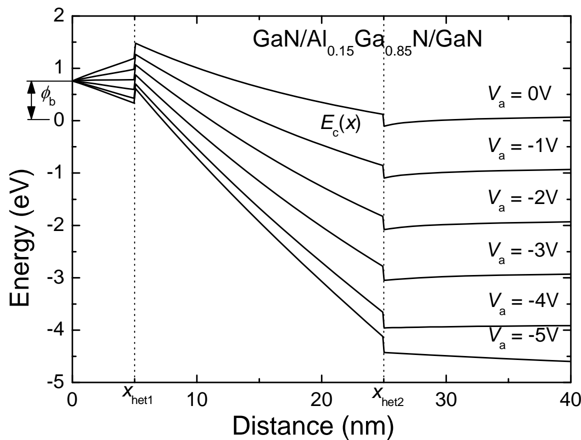

Fig. 2: *Band diagram of* metal/GaN/ /AlGaN/GaN *heterostructures with Schottky barrier height* ϕ_b=0.8 eV *at various values of reverse bias* V_a.

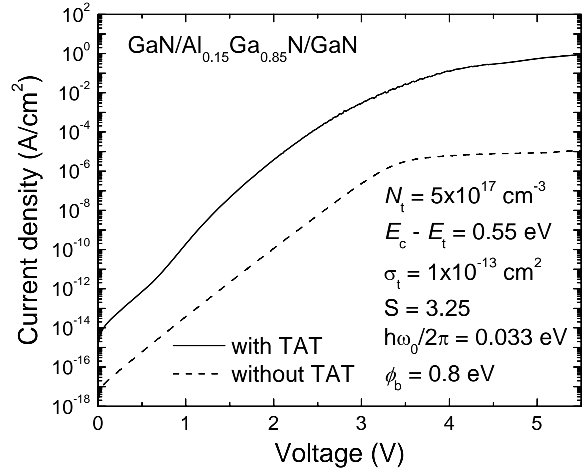

Fig. 3: *Reverse I-V curves with enabled/ /disabled model of TAT. Schottky barrier height* ϕ_b=0.8 eV, *concentration of traps* N_t=5×10^{17} cm^{-3} *at energy level* E_t lying 0.55 eV *below the conduction band, effective cross section* σ_t=10^{-13} cm^2.

Figure 2 shows the band diagram of the structure at various values of reverse bias V_a. The potential barrier of the heterostructure decreases with increasing reverse bias (while the Schottky barrier remains intact), which results in an exponential increase of current. When the barrier on the first heterojunction falls below the Schottky barrier, the reverse current saturates and its magnitude is limited by the Schottky barrier height.

Figure 3 displays *I-V* curves of the heterostructure with enabled and disabled model of TAT. The current transport due to TAT depends primarily on the material parameters of GaN and AlGaN, thus on the Huang-Rhys factor *S* and effective phonon energy $\hbar\omega_0$. The lower these values, the stronger the contribution of TAT. The TAT phenomenon depends also on the parameters of the traps, thus on the energy level, concentration and effective cross-section of the traps.

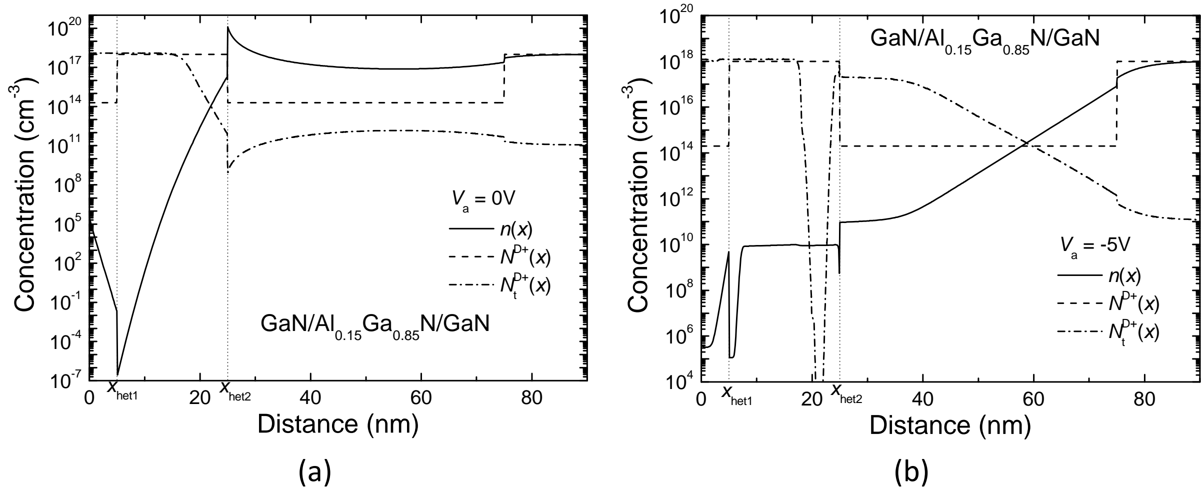

Fig. 4: *Distributions of free electrons n*(x) *and ionized deep traps* $N_t^{D+}(x)$ *in the heterostructure:* (a) *At* V_a=0 *with maximum concentration of electrons in the quantum well,* (b) *under negative bias* V_a=–5 V *pushing electrons out of the quantum well.*

Figure 4 shows the distributions of free electrons $n(x)$ and ionized deep traps $N_t^{D+}(x)$ in the heterostructure at various values of negative biases V_a. One can see that the increasing negative bias pushes electrons out of the quantum well of the two-dimensional electron gas.

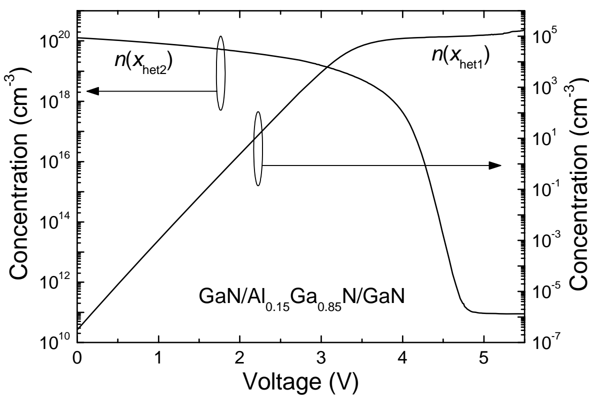

Fig. 5: *Dependence of the concentration of electrons at the first and second heterojunctions on the reverse bias.*

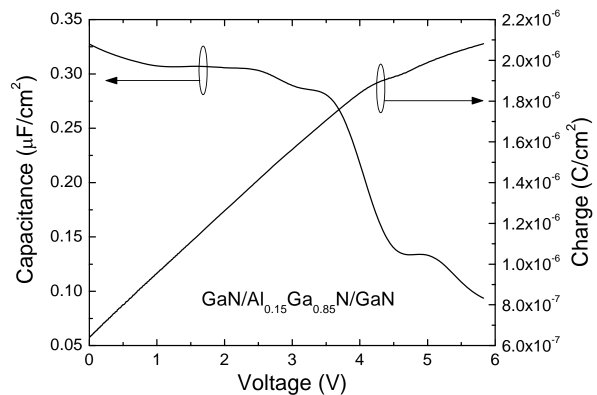

Fig. 6: *Positive sheet charge in the heterostructure in dependence on the reverse voltage. By differentiating this dependence one obtains the C-V curve.*

Figure 5 presents the dependence of the concentration of electrons at the first and second heterojunctions on the reverse bias. With increasing reverse voltage the concentration of electrons on the second heterojunction in the quantum well of the two-dimensional electron gas decreases and, vice versa, the concentration of electrons on the first heterojunction increases due to a decreasing energy barrier of the heterostructure.

Figure 6 shows the dependence of the positive sheet charge in the heterostructure in dependence on the reverse voltage. By differentiating this dependence one obtains the *C-V* curve.

3. Conclusions

The described TAT model of the metal/GaN/Al_xGaN_{1-x}/GaN structure allows analyzing the effect of deep traps upon *I-V* and *C-V* characteristics.

The negative charge with magnitude proportional to the molar concentration of aluminium gives rise to a barrier at the first heterojunction, which is higher than the Schottky barrier at the metal/GaN interface. On increasing the reverse bias V_a the barrier at the first heterojunction is getting lower. The drop of this barrier causes an exponential increase of the reverse current. The current saturates, when the first heterojunction barrier is lower than the Schottky barrier. The effect of TAT can be observed also on varying the parameters of the band of traps.

The shape of the simulated *C-V* curve is affected by changes in the charge on the second heterojunction. In principle it reflects the decrease of electron concentration in the quantum well on increasing the reverse bias V_a. The space charge region becomes wider and the electron concentration at the second heterojunction falls below the concentration of ionized deep trapping centres, which manifests itself as a noticeable drop in the capacitance of the metal/GaN/Al_xGaN_{1-x}/GaN structure.

4. Acknowledgments

The work has been supported by the Scientific Grant Agency of the Ministry of Education, Science, Research and Sport of the Slovak Republic and of the Slovak Academy of Sciences (project VEGA 1/0712/12).

5. References

[1] J. Racko, M. Mikolášek, A. Grmanová, J. Breza, P. Benko, O. Gallo, L. Harmatha: Radioengineering **21**, 213 (2012).

[2] A. Schenk: Solid-State Electronics **35**, 1585 (1992).

[3] J. Racko, M. Mikolášek, R. Granzner, J. Breza, D. Donoval, A. Grmanová, L. Harmatha, F. Schwierz, K. Fröhlich: Central European Journal of Physics **9**, 230 (2011).

[4] J. Racko, J. Pecháček, M. Mikolášek, P. Benko, A. Grmanová, L. Harmatha, J. Breza: Radioengineering **22**, 240 (2013).

[5] S. Selberherr: *Analysis and Simulation of Semiconductor Devices*, Springer-Verlag, Wien & New York, 1984.

[6] O. Ambacher, J. Majewski, C. Miskys, A. Link, M. Hermann, M. Eickhoff, M. Stutzmann, F. Bernardini, V. Fiorentini, V. Tilak, B. Schaff, L. F. Eastman: Journal of Physics: Condensed Matter **14**, 3399 (2002).

[7] N. Al Mustafa, R. Granzner, V. M. Polyakov, J. Racko, M. Mikolášek, J. Breza, F. Schwierz: Journal of Applied Physics **111**, 044512 (2012).